The Packaged and Mounted Diode as a Microwave Circuit

WILLIAM J. GETSINGER, MEMBER, IEEE

Abstract—Suitable definitions of the elements in the equivalent circuit of a packaged diode yield a lumped-element circuit with an impedance at its terminals which is the same as the total radial-line impedance of the packaged diode with the outer surface of the diode taken as the terminal surface. Consideration of the packaged diode as a radial-line structure permits an analytical justification for the incorporation of the diode circuit with the circuits of waveguide, coaxial-line, and strip-line diode mounts. As a result, the lumped-element equivalent circuit of a packaged diode can be directly related to the microwave equivalent circuit of the diode and the mount together. Diode element values, which were obtained from low-frequency measurements, have been used in conjunction with the theoretically determined circuits of mounted diodes to predict resonant frequencies at *X*-band of waveguide, coaxial-line, and stripline mounts holding packaged diodes. Similarly, antiresonant frequencies of greater than 20 Gc/s have been predicted for diodes in a radial cavity. The validity of all these predictions has been verified by measurement.

I. Introduction

THE PARASITIC elements of conventional packaged and mounted diodes may be negligible at *L*-band and lower frequencies. These parasitics become more important and are usually dominant in their effect on circuit performance at *X*-band and higher frequencies.

Thus, adequate circuit description of the packaged diode and its mount is necessary for effective design at frequencies above a few gigacycles per second, especially for broadband components such as switches or tunnel-diode amplifiers, or for components that operate with widely spaced frequencies such as a parametric amplifier usually does.

At present, the packaged diode is usually represented by a two-terminal circuit of poorly defined lumped elements, whereas we wish to have a circuit consistent with the use of the diode at microwaves. To the author's knowledge, circuits of diode mounts simply have not been discussed, whereas we need to know how the active diode elements are coupled to the terminal plane of the transmission line for which the mount is a termination.

The basic structure to be considered in this paper is that of a cylindrical diode package mounted with its axis normal to parallel metal surfaces that extend somewhat beyond the diode package. While this basic structure cannot be incorporated in all possible diode mounts, it does allow incorporation in a number of different and useful mounts, as will be described subsequently.

We will show how the equivalent circuit of the diode can be modified by appropriate definitions of case capacitance and package inductance, to be in harmony with microwave concepts. This will result in an equivalent circuit for the packaged diode that is independent of the mount in which it is used, and which can be evaluated at low frequencies.

We will then go on to show, and will justify analytically where necessary, how the diode equivalent circuit can be combined with the microwave equivalent circuit of the mount. The result will be a total equivalent circuit for diode and mount, referenced to an appropriate terminal plane in the mating transmission line. This total circuit will be useful over a very wide frequency range.

Finally, using typical 0.080-inch diameter packaged diodes from two manufacturers, measurements will be cited verifying the theoretical approach in waveguide, coaxial-line, and strip-line mounts. For a radial-line cavity, measured results will be given showing agreement with theory at frequencies beyond 23 Gc/s.

Before defining packaged-diode circuit elements and deriving appropriate equivalent circuits for diode mounts, it is desirable to mention basic concepts bearing on the problem.

II. Basic Concepts

At microwave frequencies, terms such as "impedance" and "network" have meaning only in reference to specific transmission-line modes at physically localized terminal planes. A "terminating impedance" thus terminates a specific mode on a specific type of transmission line at a specific terminal plane. A "coupling network" couples particular modes on particular transmission lines at particular terminal planes.

With this concept clearly in mind, the problem of establishing a quantitatively meaningful microwave equivalent circuit for a packaged and mounted diode becomes a problem of establishing transmission-line modes and terminal planes.

Many practical diode mounts, connecting to various types of transmission lines, have the packaged diode, a circular cylinder, mounted with its axis normal to parallel metal planes spaced by the height of the diode package. Along the surface of the diode in such a mount, the electric field lines are predominantly axial and the magnetic field lines predominantly circumferential. This

Manuscript received June 28, 1965; revised September 30, 1965.
The author is with the Lincoln Lab., Massachusetts Institute of Technology, Lexington, Mass. (Operated with support from the U. S. Air Force.)

allows matching fields to a radial line operating in its TEM mode. Thus, the diode can be considered as a terminating network for a radial line and the most natural "terminal plane" is the outer surface of the diode cartridge. Of course, this is not a plane, but a cylindrical terminal surface. Nevertheless, it is the surface required to make a meaningful definition of microwave impedance appropriate to the mode involved.

Since the diode mount is connected in some manner to a conventional transmission line, a coupling network is required between the diode terminal surface and the connecting transmission-line terminal plane.

This paper will delimit diode-package series inductance and shunt capacitance in a manner that gives the proper radial-line impedance over the surface of the diode. Then, coupling networks between diode terminal surface and transmission-line terminal plane for shunt-connected and series-connected diodes will be derived.

The use of lumped-element equivalent circuits for describing the behavior of physical components is always an approximation, since all physical circuits are, to some extent, distributed. However, the approximations can be very good for circuits confined to electrically small regions. The high-frequency limitation on lumped-element representation is usually due to the electrically large size (retardation) rather than to the distributed nature of the component. Thus, although both diodes and mounts are at least semidistributed, lumped-element representations will be used for the network between the diode junction and the transmission-line terminal plane that defines the mount.

In general, classical lumped elements are not assumed. The classical lumped element requires a field of a single type, electric or magnetic, confined to a small closed region by electric or magnetic walls [1]. We are not attempting to define lumped elements in this sense, but only to find a circuit that can be described to a very good approximation by lumped-element mathematics. To do this, we allow both electric and magnetic fields to exist within the region of circuit definition, and we allow the small region to be bounded not only by electric or magnetic walls, but also, at the terminal surface, by an immittance wall. That is to say, the fields inside the circuit defining regions are confined over the terminal surface by matching them with equal fields just outside the terminal surface. This is not an unusual approach; the same assumptions are implicit when, for example, we speak of the impedance at some terminal plane of a short length of transmission line.

A final point to clarify is that any bounded, small, well-defined, two-conductor circuit, such as a classical lumped element, or a coaxial or radial line operating in its TEM mode, has uniquely defined values of voltage and total current at its terminal surfaces, provided the fields on the terminal surface are purely tangential. Specifically, voltage V and total current I are given by

$$V = -\int_1^2 \overline{E}\cdot d\bar{l} \tag{1}$$

and

$$I = \oint \overline{H}\cdot d\bar{l} \tag{2}$$

where $d\bar{l}$ is an incremental length vector lying in the terminal surface, $\overline{E}$ is the electric field vector, and $\overline{H}$ the magnetic field vector. The integration in the voltage equation is along any path in the terminal surface connecting the conductors, designated by (1) and (2). The integration in the current equation is along any closed path in the terminal surface that encircles one conductor. The product of voltage with conjugated total current specifies stored and dissipated energy beyond the terminal surface within the defined region in agreement with Poynting's theorem, while the ratio of voltage to current specifies the impedance at the terminal surface.

When two such regions as previously described have a common terminal surface, voltage and current at the terminal surface must be the same for both regions. Now, an equivalent circuit is a shorthand way of describing relations among voltages and currents of a physical structure. Since voltages and currents are defined in the same way for all bounded, small, two-conductor physical circuits with tangential fields at their terminal surfaces, it follows that immitances determined for one such structure are mathematically compatible with the immittances determined for another such structure. Thus, if one such structure is physically joined to a different such structure, the electrical characteristics of the total new structure can be described by directly joining the equivalent circuit of the first structure to that of the second. Physical discontinuities at the interface that distort the tangential character of the fields on the terminal surfaces may be accounted for by incorporating appropriate junction susceptances.

III. Conditions and Definitions

Most diode packages used at microwaves consist of a hollow dielectric right-circular cylinder with metallic end caps that are coaxial with the dielectric cylinder. The diameters of the end caps may be larger or smaller than the dielectric cylinder, may be various thicknesses for different packages, and are often absorbed into the mounting surfaces. This leaves the dielectric cylinder as the largest regular shape common to most mounted diode packages. A cross section of a typical diode package is sketched in Fig. 1(a). Internal details are shown to help give an intuitive understanding of the packaged-diode equivalent circuit shown in Fig. 1(b) for a varactor diode. However, this paper does not concern itself with the internal construction of the packaged diode beyond assuming the existence of an equivalent circuit of suitable form to describe the electrical behavior of the struc-

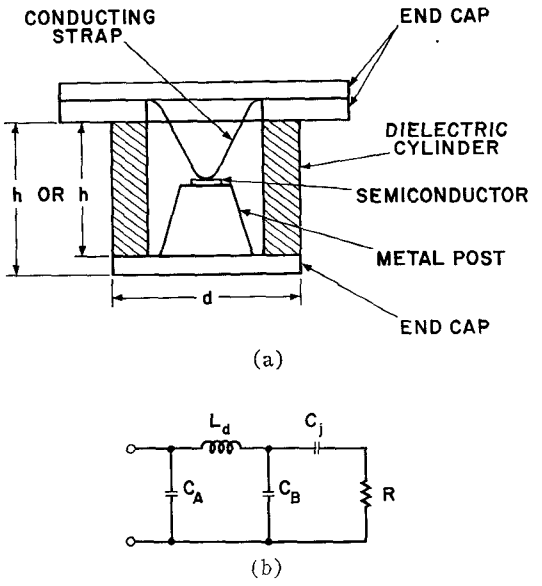

Fig. 1. Typical diode package and equivalent circuit.

ture in the frequency range where the diode package is small.

Conditions imposed in the following development are that the diode package is small in terms of wavelengths, that it is circularly cylindrical, that it is mounted between plane and parallel conducting surfaces flush with the ends of the dielectric cylinder, and that any other conducting surfaces of the mount are well removed from the vicinity of the diode. These conditions are not severely restricting because they are often met or approximated in practice.

The parallel conducting surfaces between which the diode package lies act as the conductors of a radial line external to the package. In effect, the packaged diode must couple to the radial line and the radial line must couple eventually to the terminal surface of the mount. Since TEM-mode propagation alone is assumed in the vicinity of the diode-package surface, only the circumferential magnetic field and the axial electric field at the diode-package surface are effective in coupling the diode circuit to the radial line, and thus, to the mount. It might be argued that the fields at the surface of the diode package are not purely circumferential and axial, but are distorted by peculiarities of the internal structure of the diode package and, therefore, this approach does not hold.

This objection can be overcome by considering the distorted fields to be a superposition of higher-order radial-line modes, none of which propagates if

$$2h/\lambda < 1$$

and

$$\pi d/\lambda < 1 \tag{3}$$

which inequalities usually hold in practice.

Since these modes are cut off, they represent stored energy and show up in the packaged-diode equivalent circuit as parts of the package inductance and capacitance.

In view of this, it is not necessary to have specific knowledge of the details of the internal construction of the diode package, provided an adequate equivalent circuit representation exists.

As a concrete example, the widely accepted equivalent circuit of a packaged varactor diode, as shown in Fig. 1(b), will be used in this paper. It is to be emphasized that this paper does not investigate the equivalent circuit of the packaged diode; rather, it investigates how the equivalent circuits of the diode and mount can be separated so that the diode equivalent circuit is independent of that of the mount. It further shows appropriate equivalent circuits for a variety of mounts.

It is now necessary to define diode-package capacitance and inductance so that the diode equivalent circuit will predict the proper radial-line impedance at the diode-package surface. The package inductance L_d and package capacitance C_A of Fig. 1(b) are made independent of the diode mount and, thus, unique to the package by defining them on the basis of impedance measurements made relative to the diode-package surface considered as a radial-line terminal plane.

Consider a diode mount that is electrically small at the frequency of measurement. It holds the diode package between parallel plates in accordance with the foregoing conditions. Then, using this mount, diode-package inductance L_d and capacitance C_A are defined as the circuit elements of a packaged diode having its junction region internally short-circuited. These elements are determined (formally) by impedance measurements made some distance from the packaged diode and transformed to the packaged-diode surface considered as a radial-line terminal surface.

The inductance L_d of the internally short-circuited diode package is the difference between the mount inductance measured with the short-circuited diode package in place in the mount, and the mount inductance measured with the short-circuited diode package replaced by a highly conductive dummy whose external dimensions are the same as those of the short-circuited diode package. The frequency of measurement is assumed to be low enough that capacitive effects are negligible.

This measurement is given on the basis of a lumped-element standpoint. From a transmission-line point of view, the highly conductive dummy establishes the terminal surface and an impedance measurement is made with respect to that terminal surface, thus determining L_d. This inductance is similar to excess series inductance L_{ex} of [2] or L_{min} of Hauer [3], under suitable restrictions.

The capacitance C_A can be measured approximately using an internally open-circuited diode package and the relation

$$C_A = C_A' + C_d. \tag{4}$$

Here, C_A' is the difference between the mount capacitance measured with the open-circuited diode package in place in the mount, and the mount capacitance measured with the open diode package replaced in the mount by only the end caps of the package in order to to obtain properly spaced plane, flush, and parallel surfaces within the diode-package terminal surface. The quantity C_d is the parallel-plate capacitance of that part of the mount within the diode-package terminal surface and is given by

$$C_d = \frac{\pi d^2}{4h} \epsilon_0 \tag{5}$$

where d and h are the diode-package diameter and the mount parallel-plate spacing, respectively; ϵ_0 is the absolute permittivity of air.

Considering this capacitance measurement from a transmission-line point of view, it would be desirable to terminate the diode-package terminal surface in an open circuit, but this is not possible. It is possible to terminate the terminal surface by the mount capacitance C_d within the terminal surface, and then measure the additional capacitance C_A' when the open-circuited diode is used.

The separation of C_A into C_A' and C_d is useful because these quantities will enter into the circuits for shunt-mounted diodes, as will be shown subsequently.

Package inductance and package capacitance have now been defined, and formal measuring techniques have been described. Applications to transmission-line mounted diodes will be given next.

IV. Application to Shunt-Mounted Diodes

The preceding section considered a diode as a packaged network, shown in Fig. 1(b), completely enclosed in a cylinder of diameter d and height h, as shown in Fig. 1(a). Now it is desired to find the coupling network that arises when the diode shunts a transmission line of the same height as the diode.

The most general applicable analysis is that for a dielectric post in a rectangular waveguide ([4], Sec. 5.12, p. 266–267). The generality of the analysis lies in the fact that it holds for complex values of dielectric constant. The applicability lies in the fact that the analysis describes the effect of the complex-dielectric post in terms of the radial-line admittance of the post at its surface. At a given frequency, real and imaginary parts of the post dielectric constant can be adjusted (conceptually, at least) to provide any desired value of radial-line admittance over the surface of the post. If the post were replaced with a diode of the same size and having the same radial-line admittance over its surface, it would be reasonable to expect that the waveguide equivalent circuit would be unchanged. If the diode diameter and height are small compared to a wavelength, the radial-line admittance is described by the lumped-element equivalent circuit, as mentioned previously. Thus, the equivalent circuit of a diode shunting a waveguide is given by the equivalent circuit of a dielectric post in a waveguide with the radial-line admittance of the post replaced by the diode equivalent circuit of Fig. 1(b), having diode elements defined as in the preceding section. In fact, this point of view holds only if the diode diameter is small compared to the waveguide wide dimension a. This restriction will be recognized by requiring that

$$(\pi d/a)^2 \ll 1.0 \tag{6}$$

and neglecting all terms with $(\pi d/a)^2$ as a multiplier. With reference to Sec. 5.12 [4], it can be seen that the preceding restriction allows the equivalent circuit of a dielectric post in a waveguide to be simply a reactance $-jX_a$ shunting the guide. The equation from Marcuvitz [4] for X_a can be rewritten as

$$-X_a = \csc^2 \frac{\pi x}{a} \left[\omega \frac{\mu b}{2\pi} S_0 - \frac{1/J_0^2(\pi d/\lambda)}{\frac{\pi d}{\eta b}\sqrt{\epsilon'}\frac{J_1(\pi d\sqrt{\epsilon'}/\lambda)}{J_0(\pi d\sqrt{\epsilon'}/\lambda)} - \frac{\pi d}{\eta b}\frac{J_1(\pi d/\lambda)}{J_0(\pi d/\lambda)}} \right]. \tag{7}$$

In (7) S_0 is a function that will represent an inductance in the equivalent circuit, η is the impedance of free space, ϵ' is the dielectric constant (possibly complex) of the post, b is the height of the waveguide and x is the position of the post measured from the side of the guide. Also, the appropriate definition of waveguide characteristic impedance for consistency with small-diameter TEM-mode radial-line impedance is

$$Z_0 = 2\frac{\eta b \lambda_g}{a\lambda}. \tag{8}$$

The form of (7) has been chosen to show explicitly the dependence of $-X_a$ on the radial-line admittance of the dielectric post. In the denominator of the second-term in brackets of (7), the first quantity is precisely the radial-line admittance Y_d of the dielectric post, while the second quantity is the negative of the radial-line admittance ωC_d at the post radius, but with the post absent. If the admittance Y_d is complex, $-jX_a$ should be replaced by an impedance Z_a. Using these ideas, (7) becomes

$$Z_a = \csc^2 \frac{\pi x}{a} \left[j\omega \frac{\mu b}{2\pi} S_0 + \frac{1}{Y_d - j\omega C_d} \right] \tag{9}$$

where $J_0^2(\pi d/\lambda)$ has been set to unity by virtue of the restriction of (6), and C_d is given by (5).

Equation (9) describes the impedance of the branch arm of the equivalent circuit of Fig. 2. This circuit is applied to a diode mounted in a waveguide, as shown in Fig. 3(a), simply by replacing the radial-line admittance Y_d of the post at diameter d with the radial-line admittance of the diode at diameter d. This results in the equivalent circuit of Fig. 3(b) for the diode centered $(x=a/2)$ in the waveguide. The inductance L_a is given by

$$L_a = \frac{\mu b}{2\pi} S_0 = \frac{X_a}{\omega} \cdot \tag{10}$$

If Y_d is allowed to become infinite, the post becomes a short circuit and the impedance Z_a is that of an inductive post in rectangular guide. Thus, the value of L_a is determined from the graphs for an inductive post in waveguide (Sec. 5.11 of Marcuvitz [4], p. 257–266) using (8) and (10).

The equivalent circuit for a diode-shunting coaxial line can be arrived at by an approach analogous to that used for a diode shunting a waveguide. The waveguide analysis was based on an array of dielectric posts spaced by more than one-half wavelength. Although to the author's knowledge, no analysis exists for dielectric posts spaced by less than one-half wavelength, there is no reason to believe that the equivalent circuit of Fig. 3(b) does not still hold, provided L_a is determined from the inductance of an array of metal posts spaced by less than one-half wavelength. Such an analysis is given in Sec. 5.21 of Marcuvitz [4] (p. 285–289).

Equation (1a) of Sec. 5.21 [4] will give L_a for an equiangular array of m identical posts [5] (or diodes) shunting a low-impedance coaxial line, shown for $m=2$ in Fig. 4. The value to be used for the post spacing a is

$$a = \frac{\pi(D_o + D_i)}{2m} \tag{11}$$

where D_o and D_i are the outer and inner diameters of the coaxial line. If Z_0 in (1a) is taken as the characteristic impedance of the coaxial line, then

$$L_a = X_a/\omega \tag{12}$$

and the appropriate equivalent circuit at the terminal plane is that of Fig. 3(b).

This approach also holds for balanced strip line shown in Fig. 5, but the specification of quantity a is not as simple as for coax. In general, for a single diode mounted between one ground plane and the center conductor, the value to use for a is the cutoff wavelength of the first higher-order mode that would propagate on the structure. Half of that value should be used for a pair of identical diodes mounted as shown in Fig. 5. This point of view is based on the idea that the dimension a is an electrical length and must be determined by electrical rather than purely mechanical considerations.

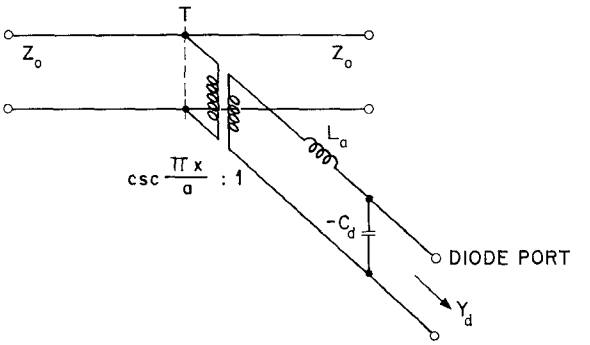

Fig. 2. Equivalent circuit for waveguide shunted by small diameter radial-line admittance.

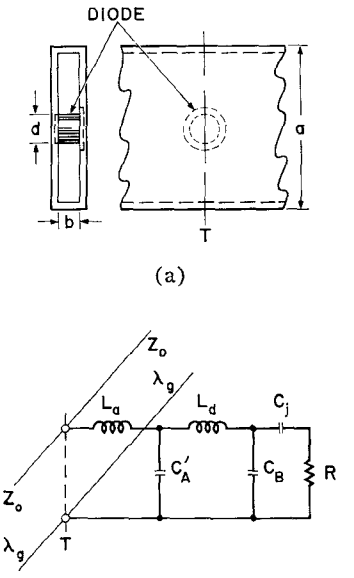

Fig. 3. Diode mounted in waveguide.

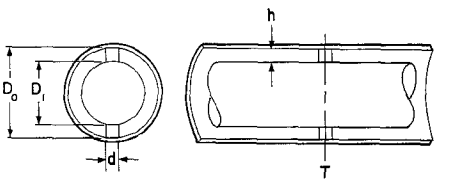

Fig. 4. Diodes mounted in shunt with coaxial line.

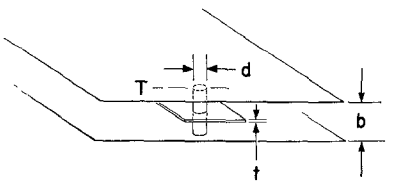

Fig. 5. Diodes mounted in shunt with strip line.

Since in waveguide and coax dimension a is identical with the cutoff wavelength of the first higher-order mode, it is reasonable to try this criterion for the more complicated cross section of strip line, involving changes of height and fringing fields. Measurements verifying the usefulness of this approach will be given in Section

VIII. It should be observed that the cutoff frequency of the lowest mode for open-sided balanced strip line is the same as the cutoff frequency of trough waveguide [6]; but the cutoff frequency of a similar strip line with closed sides (rectangular coax) is much lower, even though the side walls do not affect the dominant mode. For strip line with closed sides a more complex ridge-waveguide analysis [7] is required and two orthogonal polarizations must be investigated. However, in either situation it is fairly simple to measure the cutoff frequency by introducing a very small unbalance in the structure and finding the lowest frequency at which a sharp absorption is evident. Because the value of a used in determining L_a for strip line, or any TEM line having fringing capacitance, is not the same as the width a used to define characteristic impedance Z_0 in Sec. 5.21 of Marcuvitz [4], it is necessary to modify (1a) of Sec. 5.21 as follows: First replace the left-hand side of (1a) by L_a, and then replace the factor $a \cos \theta/\lambda$ on the right by $\mu h/2\pi$, where h, the diode height, is the same as the spacing between the center conductor and the nearest ground plane.

V. Application to Series-Mounted Diodes

The preliminary conditions required the diode to be situated between plane parallel conductors. This condition exists for a diode mounted in series with a coaxial line if the center conductor is of somewhat larger diameter than the diode. An example is shown in Fig. 6(a). Because the equivalent circuit shown in Fig. 6(b) is rather complicated, it will be discussed at some length. Later, certain circuit simplifications will be taken up. As discussed in Section II, equivalent circuits of the various small two-conductor parts of the diode and mount will be directly joined, incorporating discontinuity capacitances where necessary.

To the right in Fig. 6(b) is the diode equivalent circuit, shown as a varactor here. Next is a pi-network equivalent for the radial line extending from the diode to the diameter D_i of the inner conductor. Capacitance C_{f2}' is the fringing capacitance between the corners of the two center conductors. The two capacitances C_{f1}' are the fringing capacitances from the corner of each center conductor to the outer conductor. Finally, L_c is the coaxial inductance caused by magnetic fields in the volume bounded by the outer conductor, the two terminal planes T_1 and T_2, and the diameter D_i, where the radial line ends. The closed path defining L_c is indicated in Fig. 6(a).

If the series diode mount is terminated with a short circuit at T_2, as shown in Fig. 7, it is obvious that the appropriate equivalent circuit is that of Fig. 6(b), with C_{f1}' and T_2 short-circuited. Consideration is given next to determination of values for the circuit elements of Fig. 6(b).

The packaged-diode elements are measured by techniques to be described briefly in Section VII.

The admittance parameters of a radial-line pi-section

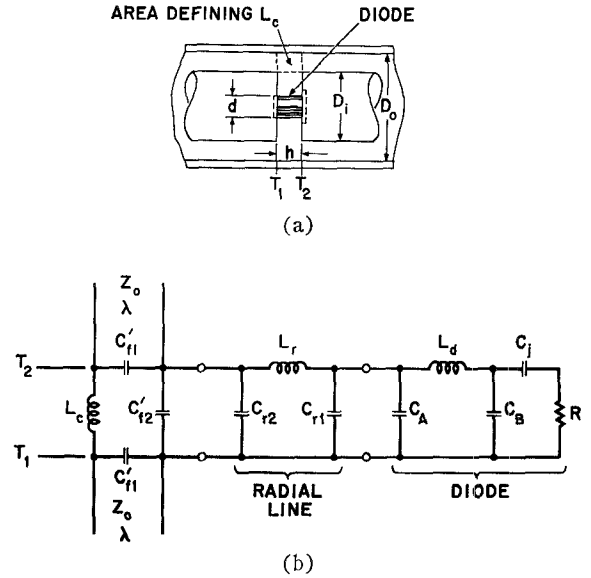

Fig. 6. Diode mounted in series with coaxial line.

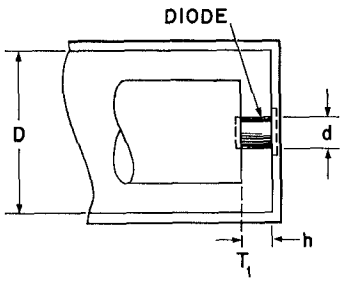

Fig. 7. Diode terminating coaxial line.

are given in Marcuvitz [4], pp. 42 and 43, and in Montgomery, Dicke, and Purcell [8], p. 268. Equation 76 in Marcuvitz [4], and (55) in Montgomery et al. [8] must be corrected by changing the explicit plus signs in the square brackets to minus signs. Also, a useful relation not stated directly in the references is

$$-ct(y, x) = \frac{Ct(x, y)}{\zeta(x, y)} \cdot \tag{13}$$

Graphs of the radial-line functions involved are given in both references and some tables are included in Marcuvitz [4].

If the radial line is less than a quarter-wavelength long, it is reasonable to assume the shunt elements are capacitances C_{r1} and C_{r2}, and the series element is an inductance L_c. Such an assumption is exact at the frequency of calculation and useful over a reasonable frequency range around the frequency of calculation, provided the radial-line length is not too close to a quarter wavelength. If diameter D_i is small in terms of wavelengths, radial-line parameters may be found in much simpler fashion from a coaxial-line approximation, which will be described in Section VI.

Approximate values for the fringing capacitance C_{f1}' and C_{f2}' can be obtained from Fig. 3 of Getsinger [9].

For the structure of Fig. 6(a),

$$C_{f1}' \simeq \pi\epsilon D_0 \frac{C_{fe}'}{\epsilon}\left(s/b = \frac{h}{D_o - d},\ t/b = \frac{D_i - d}{D_o - d}\right), \quad (14)$$

and

$$C_{f2}' \simeq \pi\epsilon D_i\left[\frac{\Delta C}{\epsilon}\left(s/b = \frac{h}{D_o - d},\ t/b = \frac{D_i - d}{D_o - d}\right) - \frac{D_i - d}{2h}\right]. \quad (15)$$

For the structure of Fig. 7,

$$C_{f1}' \simeq \pi\epsilon D_o \frac{C_{fe}'}{\epsilon}\left(s/b = \frac{2h}{D_o - d},\ t/b = \frac{D_i - d}{D_o - d}\right), \quad (16)$$

and

$$C_{f2}' \simeq 2\pi\epsilon D_i\left[\frac{\Delta C}{\epsilon}\left(s/b = \frac{2h}{D_o - d},\ t/b = \frac{D_i - d}{D_0 - d}\right) \frac{D_i - d}{4h}\right]. \quad (17)$$

Finally, the coaxial inductance L_c can be calculated from

$$L_c = \frac{\mu h}{2\pi} \ln \frac{D_o}{D_i} \quad (18)$$

for the configurations of both Fig. 6(a) and Fig. 7.

VI. Simplification of Equivalent Circuits

Since the ladder network coupling the diode junction to an accessible terminal plane may have quite a few elements, it is of interest to investigate possible simplification of the network.

The use of purely lumped elements is an approximation that will cause some small difference between actual and predicted performance of the network. The values for the diode elements will include some measurement error. Thus, if any element in the network has a series reactance or shunt susceptance very much smaller than the expected immittance at that point in the circuit, it can be neglected safely.

If two adjacent network elements, a series inductance and shunt capacitance, have small immittance, but not small enough to be neglected outright, they may often be interchanged in position. This allows them to be combined with other elements of the same type and reduces by one the number of loops in the network. Consideration of the L sections shown with their $ABCD$ matrices in Figs 8(a) and (b) indicates that the positions of L and C may be interchanged safely for frequencies satisfying the condition

$$2\omega^2 LC \ll 1.0. \quad (19)$$

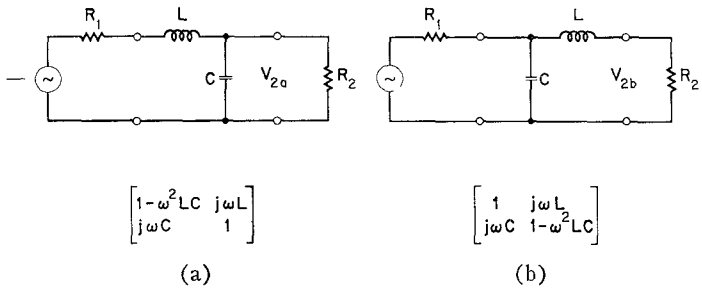

Fig. 8. L sections with positions interchanged for L and C.

The criterion of (19) is helpful in determining the conditions under which it is feasible to replace the radial-line pi-section of Fig. 6(b) by an L section whose element values are much more easily found. To do this, calculate the total parallel-plate capacitance C_r' between the ends of the center conductors in Fig. 6(a) or between the end of the center conductor and the short-circuit plane of Fig. 7 using

$$C_r' = \pi\epsilon \frac{(D_i^2 - d^2)}{4h}. \quad (20)$$

Then calculate the coaxial inductance L_r' of the radial line, using

$$L_r' = \frac{\mu h}{2\pi} \ln \frac{D_i}{d}. \quad (21)$$

Now, for the worst case, half the capacitance C_r' represents C_{r1} and half C_{r2} of the radial line indicated in Fig. 6(b). (Actually, $C_{r2} > C_{r1}$.) With this consideration in mind, apply (19); and, if

$$\omega^2 L_r' C_r' \ll 1.0 \quad (22)$$

radial-line evaluation can be avoided by eliminating C_{r1} using (20) for C_{r2} and (21) for L_r.

Another useful technique for simplifying the circuit of the series-connected diode of Fig. 6 or 7 is to move terminal plane T_1 so that it coincides with T_2, for Fig. 6, or with the short-circuit plane in Fig. 7. This eliminates L_c and C_{f1}' from Fig. 6(b), but requires that the difference between the susceptances of capacitance C_{f1}' and the capacitance over a half-diode length, $h/2$ of the coaxial line, be negligible. This is the situation when the two are nearly equal or when the line impedances are high and the diode impedance is low. Essentially, the π or L section is approximated by an equivalent length of line of the same impedance and phase characteristic as the adjoining line.

An especially interesting example of the latter occurs when the center conductor of Fig. 7 is allowed to shrink until its diameter is equal to that of the diode dielectric cylinder. This violates the initial requirement that the diode lie between parallel plates, but may cause little error if the line impedance is high. A sketch of this special situation is given in Fig. 9. The equivalent cir-

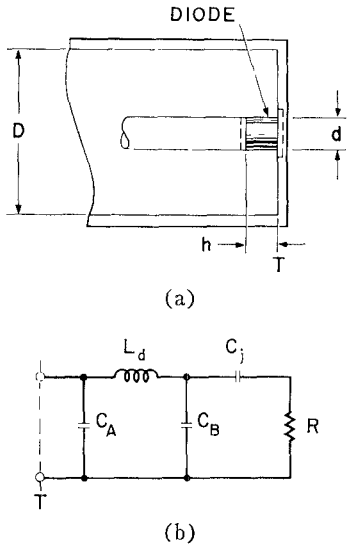

Fig. 9. Special case of diode terminating coaxial line.

cuit is found from Fig. 6(b) by observing that C_{f1}' at T_2 is short-circuited, L_c and C_{f1}' at T_1 are eliminated by moving the terminal plane T_1 to the plane of the short circuit, and the radial-line elements do not exist since there is no radial line for a center conductor whose diameter is the same as that of the diode. This leaves the equivalent circuit of the diode alone as the appropriate one for the diode and mount of Fig. 9, but only with the restriction that the coaxial terminal plane be located in the plane of the short circuit.

The price paid for this simplification is some loss of accuracy from two counts. First, the π section, consisting of L_c and C_{f1}', plus any allowable capacitance between the internal parts of the diode and the outer conductor, will have the same inductance as an equivalent length of adjoining line, but may not have the same capacitance. The effect of this is an equivalent line between T_1 and T_2 that has a different impedance and a different phase velocity than the adjoining line.

A second error is due to violation of the parallel plate constraint. The fields at the surface of the diode are no longer uniform and in phase as previously assumed. The length of the diode lies along the direction of wave propagation and the effective inductance of the diode should be treated as a length of coaxial line. This probably can be taken care of by using an approximate modified inductance L_d' at high frequencies, given by

$$L_d' = \frac{Z_o}{\omega} \tan 2\pi \frac{h}{\lambda} \approx L_d\left[1 + \frac{1}{3}\left(2\pi \frac{h}{\lambda}\right)^2\right] \qquad (23)$$

where, as before, h is the length of the diode and λ is the operating wavelength. At lower frequencies the correction term can be neglected, and at higher frequencies the correction is inadequate if the second term in brackets becomes appreciably greater than about 0.1.

Even after the equivalent circuit of a mounted diode has been simplified as much as practical, it is not at all clear from inspection alone what its transformation properties are in the frequency range of interest.

One approach to this problem is to program the network on an electronic computer, using the technique of Matthaei, Young, and Jones [10]. This approach gives the maximum quantity of numerical information, but may not provide much insight into the transformation without further analysis of the computed data.

Another approach, that is sometimes more to the point, is to determine the general circuit parameters ($ABCD$) of the network and use them directly, or to identify them with the parameters of a physically simple circuit that is more amenable to interpretation.

As an example, this approach can be used to show why varactor diode resistance measured by the DeLoach [11] method is less than the true value of the junction resistance, except for the cartridge construction used by DeLoach.

This method has the diode mounted in a waveguide, as shown in Fig. 3(a), and requires measurement of the power-transmission-loss ratio at the resonant frequency of the structure. The resistance across the guide inferred from this measurement is assumed to be the same as the diode resistance because DeLoach's equivalent circuit for the diode and mount has no shunt capacitance. This is an approximation that holds more closely for the Sharpless cartridge than for the conventional package because the point-contact connection yields no C_B, as does the welded contact; and, also, capacitance C_A' is less for the Sharpless package because it uses a quartz envelope of dielectric constant 3.8 while the conventional package uses an alumina envelope of dielectric constant 9.

However, this analysis will include both C_A' and C_B. The equivalent circuit of Fig. 3(b) between the transmission line and the arm containing the junction capacitance and resistance can be described by general circuit parameters.

When these parameters have been found, the junction impedance $R - j(1/\omega C_j)$ is used for a termination, and the real part R_m of the input impedance to the network represented by $ABCD$ is solved for. The exact result is

$$\frac{R_m}{R} = 1 \Big/ \left\{\left[1 + \frac{C_A' + C_B}{C_j} - \omega^2 L_d C_A'\left(1 + \frac{C_B}{C_j}\right)\right]^2 + [C_A' + C_B - \omega^2 L_d C_A' C_B]^2(\omega R)^2\right\}. \qquad (24)$$

The second term is usually negligible except near antiresonance. Equation (24) shows that the measured resistance R_m is equal to the diode resistance R only when both C_A' and C_B are zero; otherwise, $R_m < R$. In Section VIII, which gives measured results, typical values of R_m will be seen to be about 0.6 of R. Thus, if varactor cutoff frequency is calculated using R_m rather than R, the resulting figure is significantly higher than the true cutoff frequency.

VII. Measurement of the Packaged-Diode Circuit Elements

The details of the measurements of packaged-diode element values are too many to be included in this paper, but a brief description of the ideas used will be given.

First, for a varactor, C_j and R are determined by known methods [12]. Capacitance C_A' is measured in a mount designed in accordance with Section III, using a empty diode package and a 100 kc/s capacitance bridge. Capacitance C_d is computed from (5). Next, the total diode capacitance C_T is measured for an actual diode at the desired bias (and in the same jig). Subtractions of C_j and C_A' from C_T give C_B.

Diode inductance L_d is measured at 1000 Mc/s in a mount designed in accordance with Section III. The technique involves finding the parameters of a mathematical transformation between impedances at the diode radial-line terminal surface and at a reference plane in a coaxial slotted line. This is done experimentally by using a solid-copper dummy diode to place a short circuit at the diode terminal surface, no diode to approximate an open circuit at the diode terminal surface, and an undercut dummy diode whose inductance at the diode terminal surface can be calculated from its dimensions for a third value of terminating impedance. With the transformation determined, an internally shorted diode package is measured to find L_d.

Two diode manufacturers, MicroState Electronics Corporation of Murray Hill, N. J., and Sylvania Electric Products, Incorporated, Semiconductor Division, Woburn, Mass., generously supplied the author with a few internally shorted and empty diode packages. Average measured parameters for the packages supplied are now given.

TABLE I
Measured Diode-Package Parameters

	$L_d(nh)$	$C_A'(pF)$	$C_B(pF)$
MicroState Type 8	0.330 ±0.015	0.138 ±0.003	0.041 ±0.009
Sylvania D-5047	0.537 ±0.005	0.109 ±0.002	0.052 ±0.008

Both types of diode packages are taken as having a diameter d of 0.080 inches and a height h of 0.067 inches, which includes the smaller-diameter end cap, giving $C_d = 0.017$ pF. The tolerances given are representative of variations from package to package. Since statistically large numbers of packages were not available, these figures are tentative.

VIII. Comparison of Theoretical and Measured Performance for Mounted Diodes

Experimental justification of the theory described in preceding sections has been based in large part on resonant frequencies of a number of diodes in various mounts. The resonant frequency is unique, critically dependent on both diode and mount, and not too difficult to measure. It is also a meaningful and useful number to the component designer. Calculations of resonant frequency were made based on the equivalent-circuit element values that were measured at lower frequencies for the diodes, and computed for the diode mounts. In this section, these calculated resonant frequencies are compared with measured resonant frequencies.

In order to provide additional experimental justification of the theory, measured and calculated vlaues of effective resistance for a diode in a waveguide are compared. Finally, measured and calculated values of diode antiresonant frequency in a radial cavity are compared.

In all cases, the agreement between theory and measurement is considered by the author to validate the theoretical approach. The diodes used were gallium arsenide varactors in MicroState Type-8 packages and Sylvania D-5047 packages. The values used for the elements L_d, C_A', and C_B were the averages of those measured for short-circuited and empty packages, and given in Section VII. The diodes used were given numbers for identification and C_o and R were measured [12] and are recorded in the following. All measurements reported in this paper were made with the diodes biased at -2.0 volts dc.

TABLE II
Measured Varactor Diode Junction Parameters

Diode	$C_j(-2.0$ volts) pF	R ohms
MS # 1	0.505	1.30
5	0.376	2.20
10	0.540	1.78
19	0.423	2.00
SYL #2	0.275	2.91
3	0.480	1.17
4	0.498	1.44

It should be observed that not every diode would resonate in every jig at -2.0 volts bias within the frequency ranges for which measurements could be made.

Waveguide measurements were made using a reduced-height rectangular guide having cross-sectional dimensions of 0.060 by 0.900 inches, and with the diode mounted centrally as shown in Fig. 3(a). Although the waveguide is 0.007 inches shorter than the height of the diodes for which element values were determined, it was not believed necessary to modify the package parameters L_d and C_A' of the diode because the absorbed end cap contributes little or nothing to the values of these elements. The value for L_a was taken from Sec. 5.11 of Marcuvitz [4] and though frequency sensitive, remained within $1\frac{1}{2}$ percent of the value of 0.256 nh for all the diodes for which measurements were practical. The DeLoach [11] technique was used to make the measurements, but the tapers to reduced-height guide were not adequate for measurements below about 8.6

Gc/s. Resonant frequencies were calculated by setting diode resistance to zero and calculating the frequency of zero input impedance. This is most easily done by computer. Equation (24) was used to calculate R_m, the resistance at the waveguide terminal plane. It can be seen that R_m is appreciably less than diode resistance R, and that theory and measurement agree within a few percent. A brief discussion of the various errors involved will be given in Section IX.

TABLE III
RESONANT FREQUENCIES AND RESISTANCES FOR WAVEGUIDE-MOUNTED VARACTORS

Diode in waveguide	Calculated		Measured	
	f_0(Gc/s)	R_m(ohms)	f_0(Gc/s)	R_m(ohms)
MS # 1	8.60	—	8.52	—
5	9.77	1.33	9.38	1.33
19	9.29	1.33	9.07	1.36
SYL # 2	9.64	1.61	9.93	1.70
3	7.62	—	7.87	—

Consideration is next given to measurements on a diode shunting a length of closed, balanced strip-line (rectangular coax). The outer conductor of this line is a length of WR-51 waveguide, whose internal dimensions are 0.255 by 0.510 inches. The center conductor is a square bar 0.125 inches on a side. Thus, the spacing between the center strip and one ground plane, where the diode fits, is 0.065 inches. The characteristic impedance of this structure operating in the TEM mode is about 50 ohms. The cutoff frequency of the first higher-order mode was found to be 9.10 Gc/s by calculation [7] and 9.12 Gc/s by measurement. Thus, the value used for the dimension a was 1.295 inches. The inductance L_a was taken from Sec. 5.21 of Marcovitz [4], (observing the modifications described in Section IV of this paper), using the measured resonant frequency of each diode to determine the value a/λ needed therein. Finally, an additional inductance of 0.016 nh was added to L_a to account for a short coaxial recess that was part of the diode holder. Calculated and measured resonant frequencies, determined by minimum transmission, are given in the following table.

TABLE IV
RESONANT FREQUENCIES FOR STRIP-LINE-MOUNTED VARACTORS

Diode in strip line	Calculated f_0(Gc/s)	Measured f_0(Gc/s)
MS # 1	6.32	5.97
5	6.98	6.63
10	6.18	5.86
19	6.68	6.42
SYL # 2	7.10	7.21
3	5.99	5.97
4	5.90	5.96

Again, calculated and measured frequencies agree within a few percent, but are greatly different from those measured in waveguide. Sources of error are discussed in Section IX.

Attention is directed next to a mount having the diode in series connection. This mount is a shorted length of 50-ohm coaxial line terminated by the diode as shown in Fig. 7. The equivalent circuit is that of Fig. 6(b) with T_2 short-circuited. However, the center conductor diameter is only 0.120 inches, which is not much larger than the diode. This allows determination of the inductance L_r to be made on a coaxial-line basis as discussed in Section VI. The value found for L_r is 0.138 nh. The radial-line capacitance $C_r = C_{r1} + C_{r2}$ was computed on a parallel-plate basis and found to be 0.021 pF. Half of C_r (that is, C_{r1}) was added to C_A in the equivalent circuit, and the other half C_{r2} located on the diode side of L_c. Fringing capacitance C_{f2} was assumed to be zero. An approximate value of fringing capacitance C_{f1} from the end of the coaxial line to the outer conductor was found to be 0.011 pF. On the basis of an effective post diameter [3], a capacitance of 0.043 pF was assumed between the inner parts of the diode and the outer conductor, and half assigned to each side of L_c. The sum of these capacitances assigned to the π-network line equivalent is 0.032 pF, which is 0.025 pF less than the value of 0.057 needed if this capacitance and L_c are to represent a continuation of the 50-ohm line. This was believed to be close enough for engineering accuracy, and so L_c and the capacitance accumulated at T_1 were removed from the equivalent circuit and replaced by a section of 50-ohm line of the same length as the diode. This allowed the terminal plane T_2 at the short circuit to be used. The total equivalent circuit at T_2 is the diode equivalent circuit of Fig. 1(b) or 9(b), with $C_r/2$ added to C_A, and inductance L_r in series at the upper terminal.

Measurements were made on a microwave bridge using two identical diode mounts. With lengths of 0.120-inch center conductor in place of a diode in both coaxial mounts, a wide-band null was obtained on the bridge. With a diode replacing such a length of center conductor in one mount, a null was observed (with an attenuation adjustment to allow for diode resistance) only at resonance.

Calculated and measured resonant frequencies for diodes in the coaxial mount are given in the following table:

TABLE V
RESONANT FREQUENCIES FOR COAXIAL-LINE-MOUNTED VARACTORS

Diode in coax mount	Calculated f_0(Gc/s)	Measured f_0(Gc/s)
MS # 1	9.82	9.30
5	11.18	10.58
10	9.53	8.85
19	10.62	10.13
SYL # 3	8.35	8.30
4	8.22	8.45

These calculations do not account for the fact that the π section removed to simplify the network was not a

very good approximation for a 50-ohm line. If assumed approximations are reasonably close, the π section represented a line having a characteristic impedance of 66.6 ohms and a phase velocity 33 percent greater than that of light. These figures can be used to predict that the resonant frequency measured on the bridge mentioned above would be about two percent lower than the calculated frequency.

Also, since the center conductor was not much larger than the diode diameter, the parallel-plate restriction was probably violated to some extent. But, because the extent of this effect is not clear, (23) was not applied in these calculations. The result of the effect would be to lower the measured resonant frequency below the calculated frequency by about two percent at 10 Gc/s at most. A further discussion of errors will be given in Section IX.

The last set of measurements to be described relates measured and calculated values of antiresonant frequency for diodes in a radial cavity. This is an important example because it illustrates the usefulness of the concepts of this paper at frequencies which might ordinarily be thought too high for lumped-element techniques. In fact, the favorable geometry of the mount and the mode involved contribute greatly to the effectiveness of the theoretical approach. The antiresonant frequency of the diode alone, considered as a radial-line termination, can be calculated using the circuit of Fig. 1(b). The radial-line cavity is simply a round pillbox of the same height as the diode. In appearance it is like Fig. 7, with the coaxial inner conductor enlarged in diameter so that it contacts the outer conductor. The diameter of this cavity is designed to present an open circuit at the diode terminal surface near the diode antiresonant frequency. If diode and cavity are antiresonant at the diode terminal surface at different, but not greatly different, frequencies, the antiresonant frequency of the total structure will be somewhere between the individual antiresonant frequencies. It is the antiresonant frequency of the total structure that will be reported on.

Perhaps it should be observed that the lumped-element approach used would probably not work very well at very high frequencies for the coaxial structure of Fig. 9(a) because the length of the diode lies in the direction of wave propagation and is an appreciable portion of a wavelength. Also, trouble might be expected using the lumped-element approach at very high frequencies with the waveguide mount of Fig. 3(a) because the diameter of the diode would be appreciable compared to the width of the waveguide, and the restriction of (6) would be violated. However, for a radial-line structure, only the radius of the diode is in the direction of propagation, and the fields are uniform and in phase over the length of the diode surface.

Antiresonant frequency of the total structure was calculated as follows. First, diode resistance was neglected. Then the antiresonant frequency f_{10} and slope parameter b_1 of the diode at its terminal surface were calculated from the equivalent circuit of Fig. 1(b). Next, the antiresonant frequency f_{20} and slope parameter b_2 of the radial cavity were calculated at the diode terminal surface. To do this, an effective diameter of the cavity was measured by finding the frequency of absorption with the diode absent. It was necessary to do this rather than use the geometrical diameter in order to allow for the effects of the bias filter and coupling aperture perturbations. The physical diameter of the cavity was 0.498 inches and its electrical effective diameter 0.464 inches. The antiresonant frequency f_{20} of the cavity at the diode terminal surface was 20.5 Gc/s. Its slope parameter b_2 was 22.05 mmho. With this information, the antiresonant frequency f_{00} of the total structure was found from

$$f_{00} = \frac{f_{10}}{1 + b_2/b_1} + \frac{f_{20}}{1 + b_1/b_2}. \tag{25}$$

Results are given in the following table:

TABLE VI
ANTIRESONANT FREQUENCIES FOR RADIAL-CAVITY-MOUNTED VARACTORS

Diode in Radial Cavity	Calculated			Measured
	f_{10}(Gc/s)	b_1(mmho)	f_{00}(Gc/s)	f_{00}(Gc/s)
MS # 1	25.2	31.6	23.3	23.0
5	26.1	34.8	23.9	23.1
10	25.0	30.9	23.1	22.7
19	25.7	33.4	23.6	23.0
SYL # 2	22.8	25.0	21.7	22.6
3	21.6	21.1	21.0	21.3
4	21.5	20.9	21.0	21.5

Measurements of antiresonant frequency were made by searching for a bias-sensitive absorption of a swept microwave signal loosely coupled to the radial-line cavity. Measured and calculated results agree as well here as at lower frequencies, indicating that the frequency limit of the lumped-element approach has not yet been reached.

IX. Consideration of Errors

A graphical illustration of the errors between calculated and measured resonant frequencies for the different diodes in the various mounts is given in Fig. 10. Error ϵ has been defined by

$$\epsilon = \frac{f_0(\text{calc})}{f_0(\text{meas})} - 1. \tag{26}$$

Accuracy of measured values is only about $\pm\frac{1}{2}$ percent. The reason for this is that diode Q is relatively low and ripples in the detected signal, caused by multiple reflections in the equipment and imperfect leveling, make it difficult to define the center frequency of the resonance curve.

There are also mechanical factors causing error. Some of these are caused by small defects and dimensional errors in the diode-holding jigs. Others are due to differ-

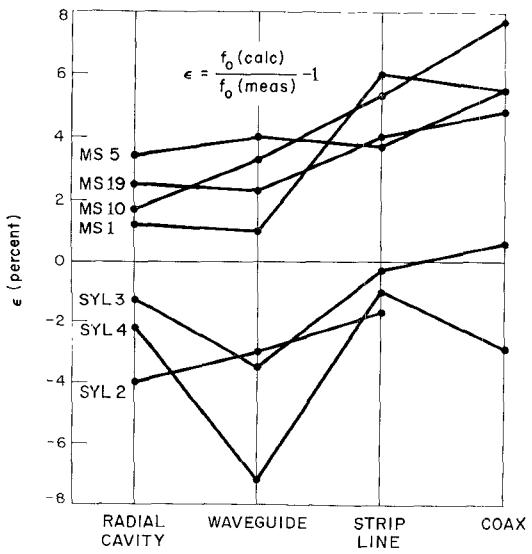

Fig. 10. Graphical presentation of errors.

ent diode lengths and also lack of concentricity and parallelness of the diode package end caps. In addition, there are differences in the internal structure from diode to diode of the same manufacturer. The results of these sources of error show up in Fig. 10 as scatter in the results for any one diode mount for diodes from the same manufacturer.

No appreciable error would be expected to be caused by the radial cavity and the waveguide mounts and so the positive average error for the MicroState diodes and the negative average error for the Sylvania diodes is probably caused by some fixed error in evaluating diode, rather than mount, elements. The reason for these errors is not understood. It may be that the short-circuited and empty packages, acquired more recently than the diodes, are not closely representative of the packages or manufacturing techniques used when the diodes were made. Or, it may be some shortcoming of element-value measurement techniques.

This same diode element-value error would be expected for the measurements in coax and strip line; however, errors due to the mount are involved here as well. Two problems that would increase the error in a positive direction for the coaxial mount were discussed in Section VI; these are inaccurate transformation of the terminal plane and violation of the parallel-plate mount restriction. The total of these errors was estimated at between two and four percent in Section VIII, and this estimate is borne out by Fig. 10. The increased positive error for the strip-line mount is also probably caused by violation of the parallel-plate restriction because the width of the strip (0.125 inch) is not much larger than the diameter of the diode (0.080 inch). It might also be observed that Sec. 5.21 of Marcuvitz [4], from which the dominant inductance L_a was found, claims of its error only that it is less than ten percent.

In consideration of the many possible sources of error in measurements, diodes, and mounts, it is believed that the agreement of the calculations with the measured values is remarkably good. There is still room for improvement, however, especially in the areas of the manufacturing of diodes and packages that are more nearly the same from unit to unit, and in the more accurate determination of packaged-diode equivalent-circuit element values.

X. Conclusion

Packaged and mounted diodes have been considered from a microwave circuit basis, and lumped-element equivalent circuits arrived at. These equivalent circuits accurately predict diode behavior over a wide frequency range and allow the designer to determine how different mounts will modify the performance of a device using a given diode. Most important, use of the mount-independent definitions for package capacitance and inductance makes it possible to design diode-using components with much less cut and try since the electrical behavior for a variety of mounts is more realistically predictable on paper.

Acknowledgment

The author wishes to express his appreciation to the many engineers from various organizations who showed an interest in this work, made many valuable suggestions, and asked pertinent questions that helped develop this paper from first intuitive concepts. The author especially thanks his colleague, F. Dominick, for his interest and for supplying equipment, diode mounts, and measurements of junction capacitances and resistances. The many other measurements and debugging problems were very ably handled by T. E. Maggiacomo.

References

[1] D. T. Paris and F. K. Hurd, "Relaxation properties of fields and circuits," *Proc. IEEE*, vol. 53, p. 153, February 1965.
[2] "Definitions, symbols, and methods of test for semiconductor tunnel (Esaki) diodes and backward diodes," *IEEE Standards* No. 253, December 1963.
[3] W. Hauer, "Definition and determination of the series inductance of tunnel diodes," *IRE Trans. on Electron Devices*, vol. *ED-8*, pp. 470–475, November 1961.
[4] N. Marcuvitz, *Waveguide Handbook*. Radiation Lab. Ser., vol. 10. New York: McGraw-Hill.
[5] C. E. Muehe, "The inductive susceptance of round metal posts mounted in coaxial line," Group Rept. 46–32, Lincoln Lab., M.I.T., November 5, 1958.
[6] K. S. Packard, "The cutoff wavelength of trough waveguide," *IRE Trans. on Microwave Theory and Techniques (Correspondence)*, vol. MTT-6, pp. 455–456 October 1958.
[7] H. G. Unger, "Die Berechnung von Steghohleitern," *Arch. elekt. Übertragung*, vol. 9, p. 157 April 1955.
[8] C. G. Montgomery, R. H. Dicke, E. M. Purcell, *Principles of Microwave Circuits*, Radiation Lab. Ser., vol. 8. New York: McGraw-Hill.
[9] W. J. Getsinger, "Coupled rectangular bars between parallel plates," *IRE Trans. on Microwave Theory and Techniques*, *MTT-10*, pp. 65–72, January 1962.
[10] G. L. Matthaei, L. Young, E. M. T. Jones, *Microwave Filters, Impedance-Matching Networks and Coupling Structures*, New York: McGraw-Hill, 1964, Sec. 2.13, p. 45.
[11] B. C. DeLoach, "A new microwave measurement technique to characterize diodes and an 800-Gc cutoff frequency varactor at zero volts bias," *IEEE Trans. on Microwave Theory and Techniques*, vol. MTT-12, pp. 15–20, January 1964.
[12] C. Blake and F. J. Dominick, "Transmission test method for high-Q varactors," *Microwaves*, p. 18, January 1965.